JCB Article

MUP-4 is a novel transmembrane protein with functions in epithelial cell adhesion in *Caenorhabditis elegans*

Leexan Hong,[1] Tricia Elbl,[1] James Ward,[1] Clara Franzini-Armstrong,[1] Krystyna K. Rybicka,[1] Beth K. Gatewood,[2] David L. Baillie,[3] and Elizabeth A. Bucher[1]

[1]Department of Cell and Developmental Biology and [2]Department of Biology, University of Pennsylvania, School of Medicine, Philadelphia, PA 19104
[3]Department of Molecular Biology and Biochemistry, Simon Fraser University, Burnaby, British Columbia, Canada

Tissue functions and mechanical coupling of cells must be integrated throughout development. A striking example of this coupling is the interactions of body wall muscle and hypodermal cells in *Caenorhabditis elegans*. These tissues are intimately associated in development and their interactions generate structures that provide a continuous mechanical link to transmit muscle forces across the hypodermis to the cuticle. Previously, we established that *mup-4* is essential in embryonic epithelial (hypodermal) morphogenesis and maintenance of muscle position. Here, we report that *mup-4* encodes a novel transmembrane protein that is required for attachments between the apical epithelial surface and the cuticular matrix. Its extracellular domain includes epidermal growth factor-like repeats, a von Willebrand factor A domain, and two sea urchin enterokinase modules. Its intracellular domain is homologous to filaggrin, an intermediate filament (IF)-associated protein that regulates IF compaction and that has not previously been reported as part of a junctional complex. MUP-4 colocalizes with epithelial hemidesmosomes overlying body wall muscles, beginning at the time of embryonic cuticle maturation, as well as with other sites of mechanical coupling. These findings support that MUP-4 is a junctional protein that functions in IF tethering, cell–matrix adherence, and mechanical coupling of tissues.

Introduction

Cell–cell and cell–extracellular matrix (ECM)* interactions are mediated by junctional complexes such as hemidesmosomes and adherens junctions. These junctions are necessary for multicellular animals to maintain the integrity of individual cells and to integrate tissue functions. Transmembrane proteins at junctional complexes, such as integrin and dystroglycan, link ECM components to intracellular cytoskeletal networks of microfilaments, microtubules, and intermediate filaments (IFs). These interactions are regulated, and defects in components of junctional complexes can affect the integrity and function of the cell, or the coordinated functions of tissues, including accommodation of mechanical forces and the assembly of ECM (Campbell, 1995; Vidal et al., 1995; Henry and Campbell, 1998; Fuchs and Yang, 1999).

This paper investigates the contributions of the *mup-4* gene to the muscle and epithelial tissue functions in *C. elegans*. Body wall muscle and the hypodermis are an excellent model to study coordinated tissue interactions. The hypodermis is a specialized epidermis that secretes a complex matrix, the cuticle, which is modified throughout the life of the worm (Cox et al., 1981; Sulston et al., 1983; Cox and Hirsh, 1985; Priess and Hirsh, 1986; Waterston, 1988; Costa et al., 1998; Hresko et al., 1994, 1999; Johnstone, 1994, 2000; Kramer, 1997; Moerman and Fire, 1997; Williams-Masson et al., 1997, 1998). During midembryogenesis, the hypodermis migrates to enclose the ovoid embryo, which then elongates three- to fourfold (threefold stage) (Sulston et al., 1983; Williams-Masson et al., 1997; Chin-Sang and Chisholm, 2000). Commensurate with embryo elongation are specific interactions between the hypodermis and body wall muscle cells, which lie in two dorsal and two ventral strips extending the length of the animal just below the hypodermis (Figs. 1 and 2 A) (Waterston, 1988; Hresko et al., 1994). These hypodermal regions are greatly flattened with elaborate IF structures, appearing similar to vertebrate

Address correspondence to Elizabeth A. Bucher, Department of Cell and Developmental Biology, University of Pennsylvania, School of Medicine, Philadelphia, PA 19104-6058. Tel.: (215) 898-2136. Fax: (215) 898-9871. E-mail: bucher@mail.med.upenn.edu

Leexan Hong and Tricia Elbl contributed equally to this work.

*Abbreviations used in this paper: ECM, extracellular matrix; GFP, green fluorescent protein; IF, intermediate filament; IFAP, IF-associated protein; RNAi, RNA interference; SEA, sea urchin enterokinase; TnT, troponin T; vWFA, von Willebrand factor A module; WT, wild-type.

Key words: filaggrin; intermediate filaments; hemidesmosomes; cell adhesion; muscle force transmission

The Journal of Cell Biology, Volume 154, Number 2, July 23, 2001 403–414
http://www.jcb.org/cgi/doi/10.1083/jcb.200007075

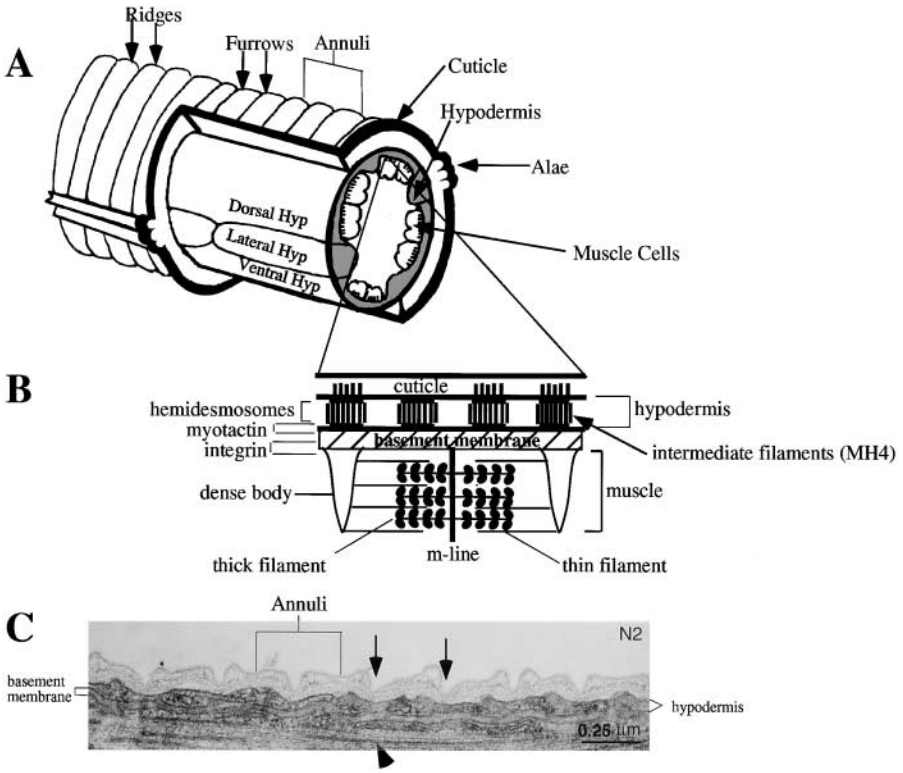

Figure 1. **Disposition of muscle and hypodermal tissues in *C. elegans*.** (A) Diagram of a cross-section of an adult worm illustrating the muscle–hypodermal-cuticular relationships, which are established by the end of embryogenesis (adapted from Costa et al., 1997). (B) Schematic diagram of the relationship of a body–wall muscle sarcomere and overlying hypodermis (adapted from Hresko et al., 1994). (C) EM of N2 worm illustrating the annuli ridges (arrow demarcates the furrows between the ridges) and the relationship of hypodermis and muscle (arrowhead).

epithelial tonofilaments. IFs are the most diverse of the cytoskeletal components and function as structural integrators of the cytoplasm to resist and transmit mechanical stress (Bartnik and Weber, 1988; Fuchs and Cleveland, 1998; Houseweart and Cleveland, 1998; Fuchs and Yang, 1999). The hypodermal IFs are associated with dense membrane plaques and fibers extending into the ECM. These structures (also called fibrous organelles) are analogous to vertebrate hemidesmosomes (Francis and Waterston, 1991), cell–matrix junctions that provide adhesive spotwelds between the IF cytoskeleton and the ECM. IFs are regulated by IF-associated proteins (IFAPs), and specific IFAPs provide linkages at desmosomes (cell–cell junctions) and hemidesmosomes (Houseweart and Cleveland, 1998; Jones et al., 1998; Borradori and Sonnenberg, 1999); however, the dynamics of IFs and IFAPs in development are not well understood. In *C. elegans* embryos, it is known that the development of the hypodermal hemidesmosomes requires interactions between muscle and hypodermal cells, and thus represents a dynamic junctional complex that coordinates tissue functions, including the transmission of muscle force to the cuticle (Francis and Waterston, 1991; Hresko et al., 1994, 1999; Plenefisch et al., 2000).

The *mup-4* gene (muscle position defective) has essential functions in the *C. elegans* embryonic epidermis: *mup-4* embryos arrest development either with their hypodermis failing to enclose the embryo, or during the threefold stage with defects in hypodermal cell organization and muscle cell positions (Fig. 2, B and C; Gatewood and Bucher, 1997). We now show that MUP-4 is a novel transmembrane protein composed of extracellular domains with EGF-like repeats, a von Willebrand factor A (vWFA) domain, two sea urchin enterokinase (SEA) modules, and an intracellular domain with homology to the vertebrate IFAP filaggrin. Analyses of the localization of MUP-4 and the ultrastructural lesions in mutants support the hypothesis that MUP-4 functions to tether IFs and to adhere the hypodermis to the apical ECM, thus providing a mechanical link that transmits muscle forces to the cuticle.

Results

Cloning of *mup-4*

mup-4 was previously mapped to a 0.02 map–unit interval on *LG* III (Gatewood and Bucher, 1997), and within this region resided a partial ORF with multiple EGF-like repeats (cosmid K07D8; cDNA group, CELK00028; Fig. 3 A) (Wilson et al., 1994). We examined *mup-4* alleles for polymorphisms in this candidate and found that *mup-4(s2426)* is a 0.8-kb Df (Materials and methods; Fig. 3 A). Sequence analysis of cloned PCR fragments demonstrated that nucleotides 2476–3318 were deleted (K07D8, sequence data available at EMBL/GenBank/DDBJ under accession no. L16679), and any protein product from *mup-4(s2426)* would be truncated: the Df begins at amino acid 1295 (see below) within the EGF repeat just before the first SEA domain, and results in the addition of RESREQKEVV-GYWNPVQFHFTXREAKCCRASQCVH* after amino acid 1295. Consistent with this molecular analysis, *mup-4(s2426)* appears null (Materials and methods).

Supporting this polymorphism result, introduction of either fosmid H14A12 or PCR products (some with a green fluorescent protein [GFP] tag) as transgenes rescues *mup-4* mutants (Fig. 3 A; Table I). Although the fosmid has two other predicted genes (C07H6.5 and C07H6.4), neither of these genes is present in other rescuing fragments, and cosmids leftward of this locus fail to rescue *mup-4* (Gate-

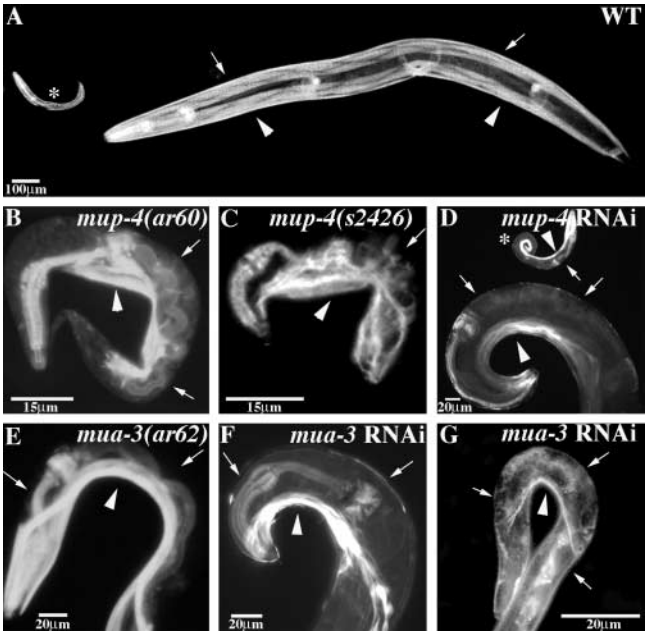

Figure 2. **Body wall muscles in WT and *mup-4* and *mua-3* mutant worms.** (A–F) Animals were fixed and stained with rhodamine-conjugated phalloidin to visualize filamentous actin and thus highlight the body wall muscles that span the length of the animal on both dorsal and ventral sides. Arrows indicate dorsal; arrowheads, ventral. (A) WT adult and L1 larva (*). *mup-4(ar60)* (B) and *mup-4(s2426)* (C) threefold-arrested embryos. Note complete displacement of dorsal muscles to the ventral side and retraction of the ventral muscles from the anterior and posterior ends. The bright muscle remaining in the head is the pharyngeal muscle. (D) Larva soaked with *mup-4* dsRNA becomes an adult with localized muscle displacement. *F_1 progeny of a soaked worm exhibiting the Mup phenotype. (E) *mua-3(ar62)* mutant larva with localized muscle displacement. (F) Larva soaked with *mua-3* dsRNA shows localized muscle displacement as an adult. (G) GFP fluorescence of the *mup-4::gfp* transgene in a Mua F_1 progeny resulting from injection of *mua-3* dsRNA into strain EE86. Note that the hypodermal *mup-4::gfp* fluorescence appears primarily localized with the displaced muscle.

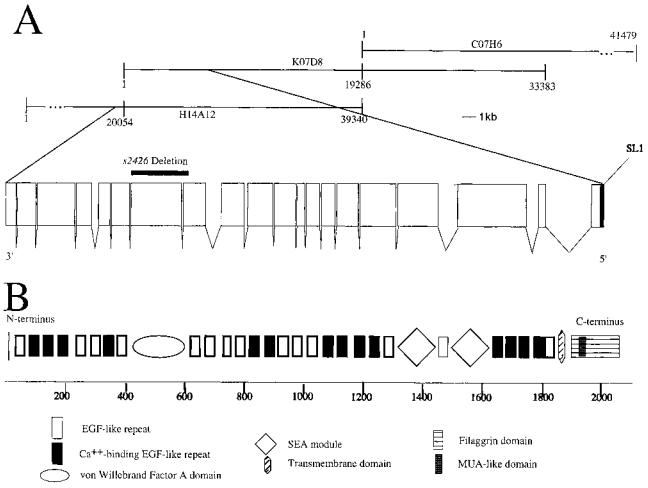

Figure 3. **(A) The localization and structure of the *mup-4* locus relative to the physical map.** The cosmids/fosmid as shown represent the actual clone boundaries. Sequences assigned to clone names in ACEDB do not reflect these boundaries. The deletion identified in the allele *mup-4(s2426)* deficiency is indicated. (B) Schematic representation of the protein structure of MUP-4 with domain key.

wood, 1996). Finally, introduction of dsRNA (Fire et al., 1998) of this ORF causes a Mup phenotype (Table II, A and B) identical to *mup-4* mutants (Fig. 2, compare B and C with D). These data establish that this ORF is *mup-4*.

MUP-4 encodes a novel transmembrane protein with a modular structure

Comparison of the cDNA and genomic sequences shows that *mup-4* has 20 exons (Fig. 3 A; cDNA, under EMBL/GenBank/DDBJ accession no. L16679). *mup-4* transcripts are transspliced to SL1, and the mature mRNA is 6739 nt encoding a predicted product of 2,104 amino acids.

Conceptual translation reveals that MUP-4 is a large transmembrane protein (Fig. 3 B). The predicted extracellular domain, composed of 1,855 amino acids, has a 15–amino acid signal peptide at the NH_2 terminus (von Heijne, 1986) followed by three distinct motifs. The first class of motif is a cysteine-rich motif (Fig. 4, legend), repeated 28 times, that is similar to the class B repeats of LDL and EGF (classification according to Herz et al., 1988). Based on conserved residues, the 28 EGF-like repeats fall into different subclasses including 27 unusual repeats, 14 with residues that mediate Ca^{2+} binding, and one of the EGF-Notch B.1 class. Except for a unique cysteine repeat 5, MUP-4 EGF-like repeats show high similarity to a *C. elegans* homologue *mua-3* (Bercher et al., 2001), with the next highest similarity often being to the Notch and Fibrillin CB-EGFs. EGF-like domains have been shown to bind other extracellular proteins (Rees et al., 1988; Engel, 1989).

A single vWFA module occurs after the eighth EGF-like repeat (Fig. 5 A). Consensus sites for Mg^{2+} binding (Lee et al., 1995), disulfide bridging, and glycosylation—three modifications typical of the vWFA domain—are found in MUP-4. Biochemical studies suggest that this domain binds to proteins such as collagen and regulates the organization of other matrix proteins (Sasaki et al., 1987; Titani and Walsh, 1988; Colombatti et al., 1993).

The final extracellular motif is the twice-repeated SEA module, separated by EGF repeat 23 (Fig. 5 B). The SEA module is associated with glycosylated proteins (Bork and Patthy, 1995), and consistent with this, MUP-4 has consensus sites for glycosylation.

After the 28th EGF-like repeat is a single pass hydrophobic segment bounded by charged residues (amino acids 1858–1882) (Argos and Rao, 1986), followed by an intracellular domain of 213 amino acids. This domain has consensus sites for phosphorylation and is homologous to an IFAP, human filaggrin (Fig. 5 C). Residues 1882–1950 are 28% similar, and the remainder are 40% similar to human filaggrin. This homology is striking since this class of IFAPs is typified by abundant phosphorylation sites and a high content of histidine, serine, glutamic acid, glycine, alanine, and arginine, often with little identifiable linear sequence homology (Steinert et al., 1981; Harding and Scott, 1983; Presland et al., 1992). The motifs found in MUP-4 are consistent with a hypothesis that MUP-4 binds to the ECM via the extracellular motifs and binds with IFs via the intracellular domain, but do not distinguish whether MUP-4 functions either in cell–cell or cell–matrix interactions.

Table I. **Transgenic rescue and expression**

Construct	Purpose	Strain injected	Lines		Injection marker	Rescue[b]
			Stable	Strains[a]		
H14A12	Genomic rescue	EE22	5	EE73	*sur-5::gfp*	full
CeMup-4.99.9	PCR rescue 2 kb upstream	EE22	2	EE74, EE75	*sur-5::gfp*	partial
CeMup-4.99.15	PCR rescue 5kb upstream	EE22	Only transients examined	0	*sur-5::gfp*	full
CeMup-4.99.1617	*mup-4::gfp* fusion rescue/expression	EE22	6	EE82	none	full
CeMup-4.99.1617	*mup-4::gfp* fusion expression	N2	4	EE69, EE86[c]	*rol-6*	—

[a]Strain name given for those lines used extensively (see Table III).
[b]For controls (see Results).
[c]Integrated line.

Distribution of MUP-4 in wild-type (WT) and mutant embryos

To determine the cellular localization of MUP-4, we examined threefold stage embryos expressing a *mup-4::gfp* transgene (Table I); since the transgene constructs rescue *mup-4(mg36)* lethality, functional MUP-4::GFP must be expressed in the correct locations. GFP fluorescence was abundant in circumferential annular rings overlying muscle of threefold embryos (not shown). The antipeptide antibody raised to the intracellular domain showed similar staining (Fig. 6, A and B). In contrast, we never observed this pattern in mutants (Fig. 6, C–F); although mutant and wild-type (WT) embryos also exhibit diffuse patterns of antibody reactivity. These data are consistent with a function in hypodermal cell–matrix junctions specifically over muscle cells.

Table II. **RNA interference studies**

A. F1 Progeny of WT adults injected with dsRNA

dsRNA	N (P_0)	% Mup	%Mua	WT	N (F_1)
buffer	5	0%	0%	100%	393
Mup-4	4	100%	0%	0%	182
Mua-3	4	0%	63%	27%	380

B. Progeny of WT L4/adults fed dsRNA

dsRNA	N (P_0)	% Mup	%Mua	WT	N (F_1)
buffer	7	0%	0%	100%	595
Mup-4	9	94%	6%	0%	711
Mua-3	14	0%	87%	13%	380

C. Effects on WT (L3 to adult) fed dsRNA

dsRNA	N (P_0)	% Mua	% WT
buffer	433	0%	100%
Mup-4	358	66%	34%
Mua-3	446	63%	37%

D. F1 Progeny of adult EE86 (*upIS1mup-4::gfp*) injected with dsRNA

dsRNA	WT	Mup or Mua	Reduced GFP	GFP+
buffer	31	0	0	100%
Mup-4	—	32	(100%)	0%
Mua-3	—	13	0	100%

N is either the number of P_0 or F_1 worms analyzed for each condition. Quantitation in A was of progeny from the second day of egg laying (earliest zygotes laid after injection do not show phenotypic effects); B was of progeny from the first day of egg laying (the phenotypic effects were less penetrant on subsequent days for fed worms); and C was of fed worms 2 d after plating. (A and B) Phenotypes were scored 2–3 d after hermaphrodite removal. The percentages represent a sum of the results from the independent P_0s. Mup mutants were scored as L1 arrested kinked worms (Fig. 2). (A and B) Mua mutants were scored as arrested Unc L1/L2 animals. (C) Mua mutants were scored as L3 adults with Unc behavior and abnormal body posture, indicative displaced muscles. Muscle displacement was confirmed by phalloidin staining in these experiments (Fig. 2). (D) Wild-type or mutant progeny were examined under a compound microscope for fluorescence. All Mup mutants resulting from injection of ds *mup-4* RNA showed absence of GFP expression, with some residual expression in the head. None of the Mua animals resulting from injection of ds *mua-3* RNA showed decreased GFP expression (e.g., Fig 2 G).

MUP-4 localization in larval and adult stages at cuticular attachment sites and to hemidesmosomes

MUP-4 continues to localize to circumferential rings over body wall muscle in larvae and adults (Fig. 7, A–C). MUP-4::

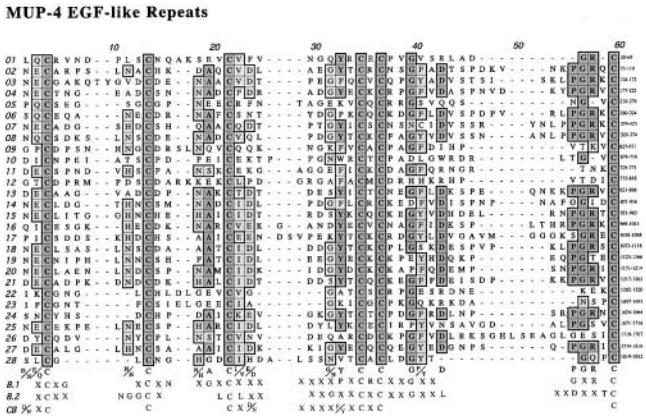

Figure 4. **Alignment of 28 cysteine-rich motifs in MUP-4.** Dark highlights indicate identical amino acids, and light highlights indicate conservative changes. The EGF motif is comprised of a characteristic pattern of six cysteines and forms a globular domain stabilized by disulfide bridges (Davis, 1990). A consensus for the MUP-4 EGF-like repeats is shown (Herz et al., 1988). The consensus specific to the Ca^{2+}-binding EGF subclass (EGF-CB) to which Mup-4 repeats 2, 3, 4, 7, 14, 15, 16, 18, 19, 20, 21, 25, 26, and 27 belong (according to Rees et al., 1988), and a consensus shared by the MUP-4 EGF-like repeats are also shown. The first 27 repeats appear as a hybrid of EGF-like classes, as defined by their spacing of six cysteines and conserved residues: before the fourth cysteine, the spacing is more like B.1, whereas after the fifth cysteine, it is more like B.2. In places where an intervening number of residues is less variant, the number most often found is listed. The position of each EGF-like motif in the amino acid sequence is shown in the last column. The juxtaposition of EGF-like domains is close, most being separated by only a few amino acids, with the exception of 67 amino acids between repeats 9 and 10. Other larger spacings reflect the interspersed vWFA and SEA domains (see Figs. 3 B and 5, A and B).

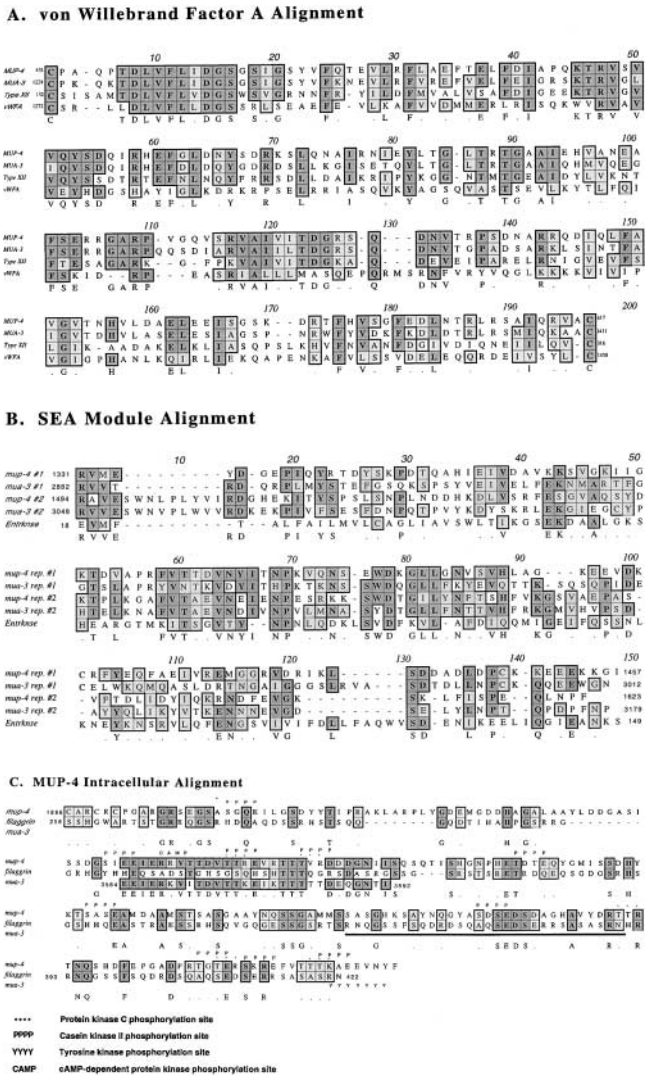

Figure 5. **Alignments of MUP-4 to the vWFA domain, SEA module, and filaggrin.** For each amino acid sequence comparison, a consensus is shown as the last line. Similarities are highlighted as described in the legend to Fig 4. (A) Comparison of vWFAs of MUP-4, MUA-3 (Bercher et al., 2001), one repeat (VA) of chicken type XII collagen (Yamagata et al., 1991), and one repeat of human vWFA (Mancuso et al., 1989). MUP-4 is most similar to MUA-3 (81%) and type XII collagen (50%). (B) Comparison of the two SEA modules in MUP-4 and MUA-3 and from enterokinase (Matsushima et al., 1994). (C) MUP-4 intracellular domain: homology to human filaggrin (Gan et al., 1990) and 30 amino acids of MUA-3 (Bercher et al., 2001). The underlined portion highlights a repeated section from filaggrin. Putative phosphorylation sites are highlighted.

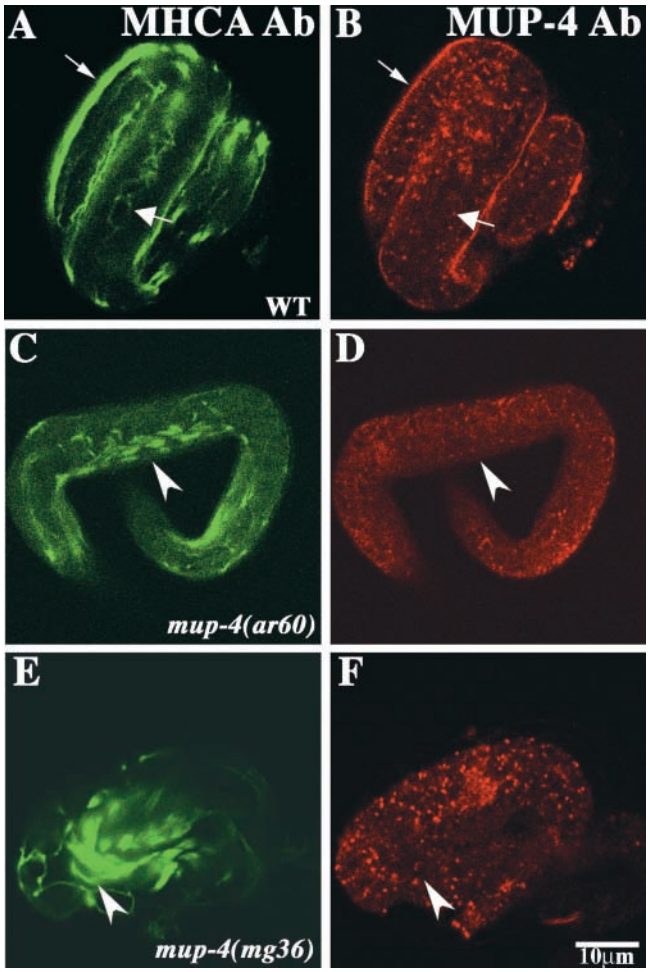

Figure 6. **MUP-4 expression in WT and mutant threefold embryos.** Triple staining patterns of the 5-6.1.1 mAb to the muscle protein myosin heavy chain A (MHCA) (A, C, and E), the MH27 mAb to epithelial adherens junctions (A, C, and E), and the MUP-4 polyclonal antibody to the intracellular domain of MUP-4. (B, D, and F) Arrows highlight the same region of the embryo. (A and B) WT embryo in which MUP-4 can be seen in some regions as circumferential rings overlying the muscle. Pharyngeal staining of MH27 is visible in A (thick arrow), whereas strong pharyngeal staining of MUP-4 is not seen in B. A background of general hypodermal cell staining is also observed in this animal. (C–F) Lateral views of *mup-4(ar60)* and *mup-4(mg36)* mutant embryos, respectively, with the characteristic muscle displacement (C and E, arrowheads). Mutants do not show the annuli-like pattern (D and F).

GFP and MUP-4 antibodies also localize to other regions where cells show mechanical attachments to the hypodermis including (a) the inner surface of the pharynx where the radial pharyngeal muscle cells attach to the marginal hypodermal cells, which secrete a cuticle; (b) overlying anal and intestinal muscles (e.g., the B cell; Fig. 7, A and B); (c) overlying vulval and uterine sex muscles; (d) male tail muscle attachment zones; and (e) the six mechanosensory neurons (Fig. 7 E) that mediate touch sensitivity through their attachment to the hypodermis (Chalfie and Sulston, 1981). Examination of WT animals also labeled with mAb MH27, which recognizes adherens junctions, shows that MUP-4 staining can extend beyond the muscle to the seam cell boundary (Fig. 7 D). In some *mup-4::gfp*-expressing lines, we often see high concentrations of protein around the hypodermal or touch neuron nuclei (Fig. 7 B; data not shown). These patterns support the mosaic analysis (Gatewood and Bucher, 1997) that MUP-4 functions in hypodermal rather than muscle cells. Furthermore, the observed pattern of MUP-4 is reminiscent of the pattern of the MH4 mAb, which recognizes IFs of hemidesmosomes (Francis and Waterston, 1985, 1991).

The relationship between MUP-4 and IF localization was further examined by overlay of confocal images of double-labeled animals. This analysis demonstrated that their patterns largely

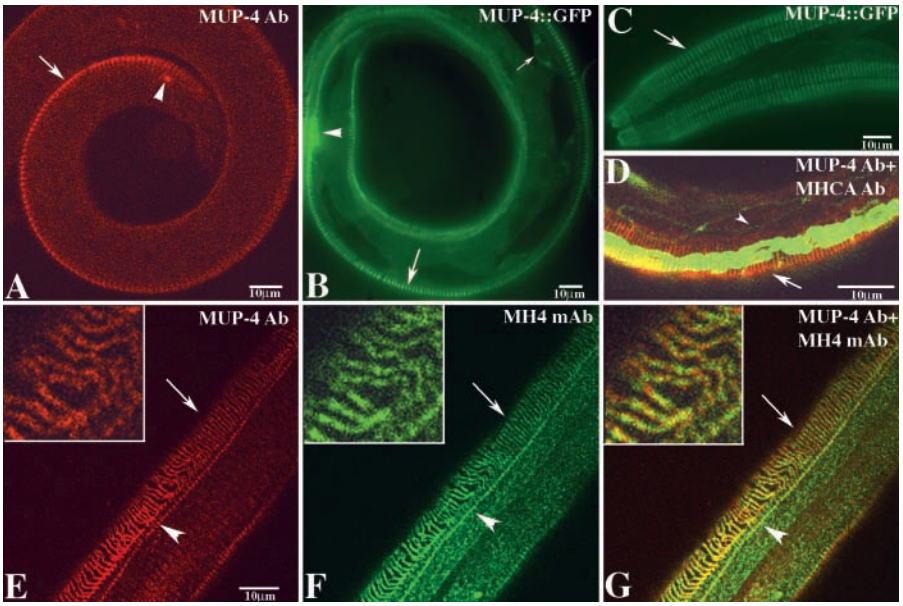

Figure 7. **MUP-4 expression in larvae.** (A) Lateral view of an N2 larva (L2) stained with a MUP-4 antibody. Arrows mark staining of MUP-4 in circumferential rings, arrowheads mark B cell perinuclear staining. (B) Lateral view of an L2 larvae MUP-4::GFP expression in an integrated *mup-4::gfp* line (EE82). Arrows mark staining in circumferential rings, arrowheads mark B cell perinuclear staining. Small arrow marks diffuse hypodermal cell staining in hypodermal cells overlying muscle. (C) Head of an L1 larva showing MUP-4::GFP fluorescence (EE73; arrow). (D) Confocal overlay of immunolocalization of MUP-4 (red) and MH27 and MHCA (green). MH27 demarcates seam cell boundary (arrowhead). (E–G) Confocal analysis of an L3 larva stained with MUP-4 and MH4 showing localization to circumferential rings (arrows) and the touch neuron (arrowheads). The confocal overlay (G) shows partial colocalization.

coincide (Fig. 7, E–G). In addition to the annular localization, MUP-4 and IF proteins are sometimes seen diffusely throughout the hypodermal syncytial cell cytoplasm, possibly reflecting protein not yet recruited to the regions overlying muscle. MUP-4 also shows coincident localization with the MH4 IF in other structures such as the touch neuron channels, further supporting that MUP-4 associates with IFs (Fig. 7, E–G).

mup-4 functions during postembryonic development

The postembryonic expression of MUP-4 suggested later developmental functions not revealed by our genetic analysis. We tested this possibility by RNA interference (RNAi) (Table II). In support of the specificity of the assay, worms treated with *mup-4* dsRNA segregate Mup progeny (Fig. 2 D, *) and injection of *mup-4* dsRNA into a *mup-4::gfp* transgene line (EE86) caused dramatic reduction in GFP expression in all Mup animals (Table II D). In contrast, worms treated with *mua-3* dsRNA segregate Mua progeny identical to *mua-3(ar62)* mutants and, when *mua-3* dsRNA is injected into the *mup-4::gfp* transgene line, all Mua progeny showed normal *mup-4::gfp* levels (Fig. 2, E–G). These RNAi data support the identity of the *mua-3* gene and that the RNAi assay is gene specific. We then soaked worms (P_0 interference) in *mup-4* dsRNA and found that MUP-4 is necessary in larvae: some larvae exhibited a phenotype within 12 h, and by 24 h, many worms were paralyzed and had displaced muscles (Fig. 2 D).

Ultrastructural analysis of *mup-4* mutants

We used transmission EM to examine the ultrastructural defects underlying the muscle displacement and hypodermal disorganization in threefold *mup-4* mutants. Micrographs of mutants demonstrated that on the dorsal surface the hypodermal cell membrane is cleanly separated from the cuticle (Fig. 8 A). Similarly, on the ventral bent surface, detachment of the hypodermis from cuticle is exhibited as giant folds of the cuticle that rise above the hypodermis, whereas the hypodermal membrane retains a straight outline (Fig. 8, A and B). We have never observed any evidence of either hypodermal cell lysis (i.e., membrane remnants associated with the cuticle), or a lesion between muscle and hypodermis (i.e., hypodermal cells associated with the cuticle with tearing at the basement membrane). In contrast, our control analysis of a *mup-2* mutant for the muscle protein troponin T (TnT)-1, in which there is abnormal muscle contraction and localized muscle detachment (Myers et al., 1996; McArdle et al., 1998), shows that the hypodermis is still attached to the cuticle (Fig. 8 C) in regions where the dorsal muscle is detached, as well as in curved ventral regions (Fig. 8 D). In contrast, all *mup-4* mutants ($n = 14$) showed a lesion between the apical hypodermal membrane and the cuticle.

Discussion

We report that MUP-4 is a novel transmembrane protein with domains consistent with its function as an IFAP at epithelial junctions. *mup-4* is expressed in the hypodermis (also see Gatewood and Bucher, 1997) and localizes to hypodermal cell–matrix boundaries, rather than cell–cell boundaries. This localization is coincident with hemidesmosome structures overlying body wall muscle, as well as at other sites of mechanical attachments of the hypodermis. MUP-4 localization develops in late threefold embryos, the stage when body wall muscle detachment occurs in *mup-4* mutants. This localization is maintained throughout development and is required, as demonstrated by RNAi. These data, and the ultrastructural studies that demonstrate a defect in attachment between the apical hypodermis and the cuticle in *mup-4* mutants, argue that MUP-4 provides a structural attachment between the epithelial cell IFs and the ECM and thereby transmits mechanical forces from the hypodermal tonofilaments to the cuticle (Fig. 1).

MUP-4 is a novel modular transmembrane protein

The MUP-4 modular structure is typical of ECM protein and matrix receptors, although aspects of this organization

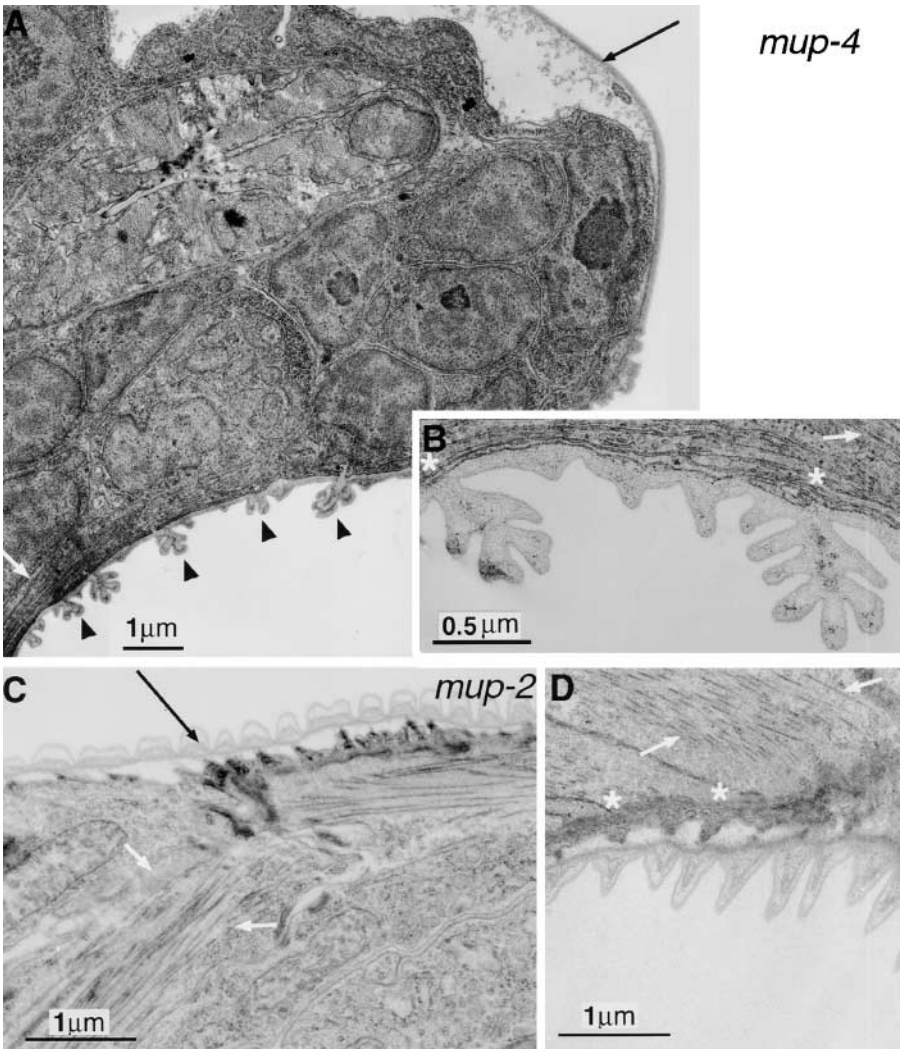

Figure 8. **Transmission EM analysis of *mup-4(ar60)* (A and B) and the *mup-2(e2346ts)* control (C and D).** Dorsal is up and ventral is down. In each panel, the white arrows highlight muscle. (A) Illustrates the characteristic appearance of a *mup-4(ar60)* mutant. On the dorsal side, the hypodermis is not attached to the dorsal cuticle (black arrow), and no muscle remains on the dorsal side. On the ventral bent surface, the cuticle is raised into large folds (arrowheads), whereas the hypodermis has a smooth outline without any obvious attachment to the folded cuticle that is normally observed (as in C and D). (B) Illustrates a typical high magnification view of the ventral surface with the arrowhead indicating the abnormal flat hypodermal surface (*) lacking attachment to the cuticle. (C) Illustrates the characteristic appearance of the dorsal surface of a *mup-2(e2346ts)/TnT-1* mutant. Displaced muscle is seen (white arrowheads) traversing the larva. Notably, the apical hypodermal membrane above this displaced muscle is still attached normally to the cuticle and densities characteristics of junctional complexes are evident (black arrow). (D) Illustrates a ventral view of a bent *mup-2* animal. In contrast to *mup-4* mutants (A and B), the ventral hypodermal membrane is not smooth, but folds upward toward the cuticle ridges. Similar to the dorsal surface, the apical hypodermis shows densities representative of junctional complexes. WT controls (Fig. 1 C; data not shown) show hypodermal–cuticle relationships similar to *mup-2* controls (Francis and Waterston, 1985, 1991).

are novel. First, 27 EGF repeats are unusual: similar EGF-like repeats have only been identified in MUA-3 and in the 63-Kd sea urchin sperm membrane protein (Mendoza et al., 1993; Bercher et al., 2001). Second, a single class B.1 EGF motif, a class associated with signaling events, occurs next to the transmembrane domain of MUP-4; although the functional significance of this organization is not yet known, it is notable that this arrangement is observed in MUA-3, and three members of the low-density lipoprotein receptor superfamily: mammalian and *C. elegans* megalin (Herz et al., 1988; Yochem and Greenwald, 1993; Yochem et al., 1999) and *C. elegans* RME-2 (Grant and Hirsh, 1999). Third, although a nonnematode homologue of MUP-4 has yet to be found, some of the motifs found in MUP-4 are observed together in other proteins (e.g., EGF and vWFA modules are found in cartilage matrix protein and integrin). The presence of EGF and vWFA modules supports the phenotypic data that MUP-4 functions in stable binding to ECM components and, based on known functions of these domains, it is possible that MUP-4 has additional functions in matrix organization and ECM cell signaling (Sasaki et al., 1987; Titani and Walsh, 1988; Engel, 1989; Colombatti et al., 1993).

A key structural feature of MUP-4 is the presence of the filaggrin domain. The filaggrin and trichohyalin class of IFAPs regulate IF compaction to generate intracellular tonofilaments during vertebrate epithelial development (Steinert et al., 1981; Rothnagel and Rogers, 1986; O'Guin et al., 1992). In differentiating epithelial cells, a highly phosphorylated propeptide of multiple filaggrin repeats, profilaggrin, is localized in keratohyalin granules. Regulated dephosphorylation controls profilaggrin processing and subsequent keratin filament aggregation (Presland et al., 1992; Haydock et al., 1993; Resing et al., 1989; Kuechle et al., 1999). This dramatic rearrangement of keratin filaments generates a squamous epithelium that is resistant to mechanical forces. Although it is conceivable that the MUP-4 single filaggrin repeat of the intracellular domain is cleaved like profilaggrin, we did not identify an obvious cleavage site. Instead, the requirement of MUP-4 in cell–matrix attachment, and the filaggrin motif within MUP-4, supports a novel association of a filaggrin domain in a transmembrane junctional protein.

Ultrastructural studies support a MUP-4 function in adhesion

The hypodermal membrane and cuticle are separated in *mup-4* mutants. In contrast, ultrastructural studies for *mup-1* (Goh and Bogaert, 1991) and *mup-2/TnT-1* (this study) mutants, which exhibit muscle detachment phenotypes grossly similar

to *mup-4,* showed normal hypodermal-cuticle disposition. Thus, detachment of the hypodermis from the cuticle is not an indirect consequence of muscle detachment, but rather a specific effect of the *mup-4* mutation. Other defects observed in the EMs for all three of these *mup* mutations, e.g., nervous system and internal organ displacement, are likely a secondary consequence of muscle/hypodermal displacement. Interestingly, our RNAi analysis of *mua-3* in the *mup-4::gfp*-expressing strain EE86 showed that the *mup-4::gfp* protein was associated with displaced muscle, consistent with a hypodermal cuticle detachment for *mua-3* mutants as well (Bercher et al., 2001). The muscle and hypodermal disorganization in threefold Mups is due to loss of linkage between the epithelium and cuticle ECM. This phenotype is analogous to lesions between the cell and basement membrane found for mutants of junctional components, including IFAPs (Jones et al., 1998) and cell–matrix receptors/adhesion proteins such as myotactin and dystroglycan (Henry and Campbell, 1998; Hresko et al., 1999).

mup-4 and *mua-3* are homologues

mup-4 and *mua-3* are homologues based on the high conservation and overall organization of EGF repeats, vWFA modules, and SEA modules (Bercher et al., 2001). For example, homologous EGF-like repeats are often ordered, the final EGF-like repeats are class B.1, and the EGF-like repeats before the vWFA domains are nearly identical. The major differences between the proteins are that MUA-3 has LDL class A repeats and nearly twice the number of EGF repeats as MUP-4. In addition, MUP-4 and MUA-3 intracellular domains have limited similarity (Fig. 5 C), although the amino acid charge distribution of the MUA-3 intracellular domain is similar to MUP-4 and filaggrins. Thus, MUA-3 may also interact with IFs (Steinert et al., 1981; Harding and Scott, 1983; Presland et al., 1992). The conserved protein structures and similar phenotypes suggest similar functions, although these functions are not redundant (see below).

MUP-4 function during development: a proposed function in IF association and hemidesmosome structure and function

Before the threefold stage, muscle is attached to the basement membrane, and microfilaments and microtubules in the hypodermis bear the internal forces of the embryo and the forces of muscle contraction during organismal elongation (Priess and Hirsh, 1986; Costa et al., 1997). Hypodermal hemidesmosomes and basement membrane components associated with muscle attachment are organized by the twofold stage (Rogalski et al., 1993; Hresko et al., 1994, 1999; Williams and Waterston, 1994; Moerman and Fire, 1997), including myotactin, a transmembrane protein that has been proposed to function at the hypodermal cell–basement membrane interface (Fig. 1 B) (Hresko et al., 1999). During the late threefold stage, there are striking transitions: (a) myotactin localization specifically to IF structures; (b) cuticle maturation; (c) reorganization of the hypodermal actin and microtubule cytoskeleton; (d) transfer of muscular forces to the cuticle; and (e) localization of MUP-4 to IF structures. These cellular transitions are essential for the mechanotransduction of muscle contraction to the maturing cuticle and to bear the internal hydrostatic forces of the worm.

A structural role for MUP-4, beginning at this critical threefold stage, is supported by the protein structure, the localization of MUP-4 to IF structures in the hypodermis overlying muscle, loss of this localization in mutants, and a lesion between the hypodermis and cuticle in mutants. Intriguingly, our antibody studies show that MUP-4 localizes to attachment structures during the late threefold stage when the cuticle is being assembled. This raises the possibility that the MUP-4 extracellular domain may be activated by secreted cuticle components, thus facilitating IF binding through dephosphorylation of the filaggrin domain. Whether or not regulation of the phosphorylation state of the filaggrin domain occurs, MUP-4 might bind to existing tonofilaments (such as that recognized by MH4) and possibly contribute in maintaining IF localization (e.g., hemidesmosomes are eventually disrupted in myotactin mutants; Hresko et al., 1999). Alternatively, the intracellular domain of MUP-4 could compact and tether other IFs (Dodemont et al., 1994; Wilson et al., 1994; The *C. elegans* Genome Consortium, 1998). Although a regulatory role has yet to be tested, a role for MUP-4 in a mechanical linkage between the cytoskeleton and the ECM is strongly supported by our data.

Cell–ECM attachments exist at the apical and basal surfaces of the hypodermis, and the MUP-4, MUA-3, and myotactin proteins each appear to be components of the hemidesmosome complex that transverses the hypodermis (Fig. 1): each exhibits similar protein localization; each has a sequence composition consistent with being IFAPs; and mutants for each of these genes have a muscle detachment phenotype. Due to their grossly similar phenotypes, we initially hypothesized that MUP-4 and MUA-3 could be stage-specific isoforms (Bucher and Greenwald, 1991; Gatewood and Bucher, 1997; Plenefisch et al., 2000); however, *mup-4* is also essential in larvae when *mua-3* functions. Although *mua-3* is expressed in embryos (Bercher et al., 2001), neither RNAi experiments, nor analysis of *mua-3(ar62)* and of *mup-4 mua-3* double mutants (Gatewood and Bucher, 1997), revealed embryonic requirements. Thus, MUP-4 appears sufficient for attachments in embryos; but during larval stages when sarcomeres are added and muscle forces increase, both MUA-3 and MUP-4 are essential. The data do not yet discriminate whether these proteins function in either the same or molecularly distinct hemidesmosomes or apically versus basally, and the thinness of the hypodermis renders differentiating apical versus basal localization impractical, even by immunogold; however, the apical hypodermal lesions in *mup-4* and *mua-3* and basal lesions in *myotactin* mutants demonstrate different functional requirements of these genes. Continued studies of these proteins should provide new insights into how these IFAPs function in IF cytoskeletal regulation, matrix interactions, and the transmission of mechanical forces during development.

Materials and methods

Worm culture

Worms (Table III) were grown according to published methods (Brenner, 1974).

Analysis of mup-4(s2426)

(*s2426)* is an allele of *mup-4* based on its map position, failure to complement *mup-4(ar60),* and segregation of Mups (Gatewood, 1996; Gatewood and Bucher, 1997; Stewart et al., 1998). Phenotypic analysis of *mup-*

Table III. **Strains**

Name	Genotype
N2	wild type
BC4636[a]	*dpy-17(e164) mup-4 (s2426) unc-32(e189); sDp3 (III;f)*
EE22	*mup-4(mg36) ncl-1(e1865) unc-36(e251); qDp3(III;f)*
EE67	*mup-2(e2346ts; him-8(e1489)*
EE69	*Ex [mup-4::gfp(CeMup-4.99.1617); rol-6(pRF4)]*
EE73	*mup-4(mg36) ncl-1(e1865) unc-36(e251); Ex [sur-5::GFP(pTG96_2) H14A12]*
EE74, EE75	*mup-4(mg36) ncl-1(e1865) unc-36(e251); Ex [mup-4(CeMup-4.99.9)]*
EE81	*dpy-17(e164) mup-4(s2426) unc-32(e189) III; sDp3 (III;f); jcIS1 IV[jam-1::gfp (pJS191) rol-6(pRF4) unc-29 (C45D3)]*
EE82	*mup-4(mg36) ncl-1(e1865) unc-36(e251); Ex [mup-4::gfp(CeMup-4.99.1617)]*
EE86	*upIs1 [mup-4::gfp(CeMup-4.99.1617); rol-6(pRF4)]*[b]
GS195	*ncl-1(e1865) unc-36(e251)glp-1(q46) mua-3(ar62); qDp3(III;f)*
GS234	*mup-4(ar60) ncl-1(e1865) unc-36(e251)glp-1(q46); qDp3(III;f)*

[a]*mup-4(s2426)* was originally named *sDf131*.
[b]Integration not mapped.

4(s2426) used a chromosomally integrated array, jcIS1 IV (provided by J. Hardin and J. Simske, University of Wisconsin, Madison, WI), which expresses JAM-1 (the MH27 antigen) at epithelial cell boundaries (Mohler et al., 1998). We constructed the strain EE81 and examined mutants under Nomarski and fluorescence microscopy. Of 326 mutants examined, 262 arrested at threefold (Mups), 14 arrested at twofold, and 44 arrested with a bean-like morphology (data not shown). These phenotypes are similar to all other *mup-4* alleles, which are variably expressed and predicted null (unpublished data; Gatewood and Bucher, 1997). The increase in early arrest over the 10% seen previously may be related to *jcIS1* IV. To identify the polymorphism, single worms were lysed at 45°C, and PCR (Williams et al., 1992) was performed using primers B0125 and B0126 (Table IV). Fragments were cloned and sequenced.

Sequence analysis

The 3′ end of the *mup-4* cDNA was determined by sequencing the 4.08-kb EST clone, yk27d6 (Kohara, 1996). 5′ sequences were generated by PCR from an N2 cDNA library (superscript II reverse transcriptase; GIBCO BRL). PCR sense and antisense primer pairs (EMBL/GenBank/DDBJ accession nos. L16679 and K07D8) were as follows: BO208 and BO187; BO211 and BO210; BO214 and BO215. The 5′ boundary of the gene was determined using BO241 and primer BO244 to the spliced leader SL1 (Krause and Hirsh, 1987; Huang and Hirsh, 1989).

mup-4 constructs for transgenic studies

Fosmid H14A12 and Cosmid C07H6 DNAs (The *C. elegans* Genome Consortium, 1998) were prepared by Cesium gradient purification (Sambrook et al., 1989). PCR fragments were generated with the expand long range PCR kit (Boeringer). CeMup-4.99.9 (10 kb) begins 1 kb upstream (BO232) from the AUG and ends 0.5 kb downstream (BO225) of the stop codon. CeMup-4.99 (14 kb) begins 5 kb upstream (B0268) from the AUG and ends 0.5 kb downstream (B0225) of the stop codon. CeMup-4.99.1617 (14 kb) begins 5 kb upstream (B0268) from the putative AUG and ends with a *gfp* reporter gene fused in frame at the *mup-4* (BO270) COOH terminus. BO273 and BO269 were used to generate *gfp* coding and *unc-54* untranslated sequences from pPD117.01 (provided by Andy Fire, Carnegie Institute of Washington, Baltimore, MD). B0270 and B0273 were hybrid primers containing *mup-4* and reporter gene sequences. The two pieces were linked by combining 1 μl of each purified fragment (Qiaquick PCR purification kit; QIAGEN) in a PCR reaction with outside primers BO268 and BO273. PCR fragments were pooled from several independent reactions, purified, and resuspended in 1× injection buffer.

Transgenic rescue and expression studies

DNAs were coinjected (20 ng/ μl) with either pTG96_2 *sur-5:gfp* (50 ng/ μl) (Yochem et al., 1998) or pRF4 *rol-6(su1006)*(80 ng/ μl) (Mello et al., 1991; Mello and Fire, 1995) into EE22 or N2. EE22 progeny inheriting the free duplication *qDp3* are phenotypically WT, whereas those failing to inherit *qDp3* are dead (Mup) (Bucher and Greenwald, 1991; Gatewood and Bucher, 1997). In the case of the *sur-5* marker, transgenic progeny were identified as GFP-positive animals and their progeny scored for uncoordinated (Unc, *unc-36* phenotype) GFP-positive animals, indicating rescue by complementation (genotype: *mup-4[mg36] ncl-1[e1865] unc-36[e251]; Ex[sur-5::gfp; H14A12]*). This was confirmed by picking Uncs and verifying that they segregated Mups and GFP-positive Uncs. For those coinjected with pRF4, the Rol phenotype was selected in addition to MUP-4:: GFP and Unc. We observed many rescued F1 progeny (not shown) and analyzed six independent transgenic lines and two independent integrated lines (integrated according to Mello and Fire, 1995).

Table IV. **Primers**

Name	Sequence
BO125	ACTATCAAGTGCGGTAACGG
BO126	GGAAGAGCATCTCCGACAGC
BO187	AGTTCTTTGCATTCGCGTCC
BO208	ACGTTCACAGTTGCCCAGC
BO210	CACACTTGTTTGTACGCCCG
BO211	CGAGTTGTTCGATATTGCACC
BO214	TGATCGTGCTGATGGGTACG
BO215	TGCTCCGGTTCTAGTGAGC
BO225	GGCGGAGCGGCCGCAGGGCCCTTCAAAACTCTTACTTTTGTTCAA
BO232	TTGGGCGCGCCTGCAGGGGATGAGGTTAAGGAAGTGACTC
BO241	CATTTGCATTCGTACC
BO244	GTTTAATTACCCAAGTTTGA
BO268	TTGGGCGCGCCTGCAGGTGAAGGAGAAGTGGACGGTGTG
BO269	AAAGCAGAAGAAGTCAACTATTTCGTACCGGTAGAAAAAATGAGTAAA
BO270	TTTACTCATTTTTTCTACCGGTACGAAATAGTTGACTTCTTCTGCTTT
BO273	AAAAAAAGGCCTTTTGGG
BO300	CAATGCCGAGTAAACGACCCACTAGTACCGGTAGAAAAAATGAGTAAAGGA

RNA-mediated interference

RNA was synthesized, using the RiboMAX large scale RNA production system (Promega), and annealed (Fire et al., 1998). *mup-4* and *mua-3* dsRNAs were generated from yk27d6 (4.08 kb) and yk360c5 (2.4 kb), respectively. Young adult hermaphrodites, either N2 or EE86, were injected with either dsRNA (150 μg/ml) or 1× injection buffer alone, plated clonally, and transferred daily (Table II).

For RNAi soaking experiments), staged worms were washed with M9 buffer. 25 μl of concentrated worms were aliquoted into siliconized tubes, to which 25 μl of either dsRNA (300 μg /ml) or 1× injection buffer were added and placed on a nutator at 22°C overnight and then plated. Individual hermaphrodites were transferred clonally 6 h later and then transferred daily (Table II).

MUP-4 antibody

The MUP-4 antibody was raised against the peptide, cysteine-linked-PRAKLARPLYGDEMGDD, from the unique intracellular domain (Fig. 5 C). The peptide and rabbit polyclonal antibody were contracted from Quality Control Biochemicals and affinity purified.

Staining

Phalloidin staining was as described (Gatewood and Bucher, 1997). For antibody staining, some embryos were harvested by treatment with a 1:10 dilution of commercial bleach in 1N NaOH and fixed (Miller and Shakes, 1995); however, the cuticle renders worms impermeable, beginning at the late threefold stage. Thus, analysis of mutants and some N2 worms was performed by the method described previously (Finney and Ruvkun, 1990; Miller and Shakes, 1995). Fixed worms were incubated with the following primary antibodies: MUP-4 rabbit polyclonal, 1:500; mouse mAb MH4 to a *C. elegans* IF, 1:125; mouse mAb 5-6.1.1 to *C. elegans* myosin heavy chain A, 1:100; and rabbit polyclonal Living Colors™ (8367-1; CLONTECH Laboratories, Inc.) to GFP, 1:200.

Microscopy

Fluorescence was analyzed either with a Leica DAS microskop DMR camera containing a Eastman Kodak Co. KAF-1400 chip, 1317 × 1035 resolution (Princeton Instruments), or as described previously (Gatewood and Bucher, 1997). Confocal images were gathered using a ZEISS Axiovert 100M with a C-Apochromat 63× water-corrected lens using LSM510 v2.02 software.

Electron microscopy

mup-4(ar60), mup-2(e2346ts) (Myers et al., 1996), and N2 worms were sequentially fixed in 2% OsO_4 (3.5% glutaraldehyde and 2% OsO_4 again) and in 0.1 M Na cacodylate buffer, pH 7.2–7.4 for 1 h at room temperature, with three washes in cacodylate buffer between fixatives. The worms were en bloc stained with 1% uranyl acetate in 70% ethanol overnight at room temperature. Worms were then washed in buffer, postfixed in 2% OsO_4 in cacodylate buffer for 1 h at room temperature, and en bloc stained in saturated aqueous uranyl acetate for 1 h. Samples were embedded in epon, and ultrathin sections were stained with 3% uranyl acetate in 50% ethanol, and with lead salts (Sato, 1985). 22 sectioned animals were examined in a Philips 410 EM: four were necrotic and disregarded; four appeared to be WT heterozygous siblings; and fourteen were mutants.

We thank A. Coulson, S. Chissoe, J. Speith and R. Wilson of the *C. elegans* Genome Consortium for clones and sequence data; Y. Kohara for EST clones; J. Plenefisch, M. Hresko, and J. Hardin for sharing unpublished data and stimulating discussions; D. Miller and R. Waterston for providing antibodies; A. Fire for vectors; J. Hardin and J. Simske for the *jam-1::gfp* transgene line; C. Emerson and D. Standiford for use of their microscope; J. Murray and Y. Vechlivich for confocal assistance; and M. Sundaram, T. Allen, J. Yochem, S. Dinardo, and J. Lok for helpful discussions. Some strains used were provided by the *Caenorhabditis elegans* Genetics Center.

Grants from the University of Pennsylvania Research Foundation and National Institutes of Health to E.A. Bucher, a National Science Foundation graduate research fellowship to T. Elbl, National Institutes of Health predoctoral training grants to B.K. Gatewood, and a grant from National Sciences and Engineering Research Council of Canada to D.L. Baillie supported this work.

Submitted: 18 July 2000
Revised: 8 June 2001
Accepted: 14 June 2001

References

Argos, P., and J.K. Rao. 1986. Prediction of protein structure. *Methods Enzymol.* 130:185–207.

Bartnik, E., and K. Weber. 1988. Intermediate filaments in the giant muscle cells of the nematode *Ascaris lumbricoides*; abundance and three-dimensional complexity of arrangements. *Eur. J. Cell Biol.* 45:291–301.

Bercher, M., J. Wahl, B. Vogel, X. Lu, E.M. Hedgecock, and J.D. Plenefisch. 2001. *mua-3*, a gene required for mechanical tissue integrity in *Caenorhabditis elegans*, encodes a novel transmembrane protein of hypodermal attachment complexes. *J. Cell Biol.* 154:415–426.

Bork, P., and L. Patthy. 1995. The SEA module: a new extracellular domain associated with O-glycosylation. *Protein Sci.* 4:1421–1425.

Borradori, L., and A. Sonnenberg. 1999. Structure and function of hemidesmosomes: more than simple adhesion complexes. *J. Invest. Dermatol.* 112:411–418.

Brenner, S. 1974. The genetics of *Caenorhabditis elegans*. *Genetics*. 77:71–94.

Bucher, E., and I. Greenwald. 1991. A genetic mosaic screen of essential zygotic genes in *Caenorhabditis elegans*. *Genetics*. 128:281–292.

Campbell, K.P. 1995. Three muscular dystrophies: loss of cytoskeleton-extracellular matrix linkage. *Cell.* 80:675–679.

The *C. elegans* Genome Consortium. 1998. Genome sequence of the nematode *C. elegans*: a platform for investigating biology. *Science*. 282:2012–2018 (errata published 283:35, 283:2103, and 285:1493).

Chalfie, M., and J. Sulston. 1981. Developmental genetics of the mechanosensory neurons of *Caenorhabditis elegans*. *Dev. Biol.* 82:358–370.

Chin-Sang, I.D., and A.D. Chisholm. 2000. Form of the worm: genetics of epidermal morphogenesis in *C. elegans*. *Trends Genet.* 16:544–551.

Colombatti, A., P. Bonaldo, and R. Doliana. 1993. Type A modules: interacting domains found in several non-fibrillar collagens and in other extracellular matrix proteins. *Matrix.* 13:297–306.

Costa, M., B.W. Draper, and J.R. Priess. 1997. The role of actin filaments in patterning the *Caenorhabditis elegans* cuticle. *Dev. Biol.* 184:373–384.

Costa, M., W. Raich, C. Agbunag, B. Leung, J. Hardin, and J.R. Priess. 1998. A putative catenin-cadherin system mediates morphogenesis of the *Caenorhabditis elegans* embryo. *J. Cell Biol.* 141:297–308.

Cox, G.N., and D. Hirsh. 1985. Stage-specific patterns of collagen gene expression during development of *Caenorhabditis elegans*. *Mol. Cell. Biol.* 5:363–372.

Cox, G.N., S. Staprans, and R.S. Edgar. 1981. The cuticle of *Caenorhabditis elegans*. II. Stage-specific changes in ultrastructure and protein composition during postembryonic development. *Dev. Biol.* 86:456–470.

Davis, C.G. 1990. The many faces of epidermal growth factor repeats. *New Biol.* 2:410–419.

Dodemont, H., D. Riemer, N. Ledger, and K. Weber. 1994. Eight genes and alternative RNA processing pathways generate an unexpectedly large diversity of cytoplasmic intermediate filament proteins in the nematode *Caenorhabditis elegans*. *EMBO J.* 13:2625–2638.

Engel, J. 1989. EGF-like domains in extracellular matrix proteins: localized signals for growth and differentiation? *FEBS Lett.* 251:1–7.

Finney, M., and G. Ruvkun. 1990. The Unc-86 gene product couples cell lineage and cell identity in *C. elegans*. *Cell*. 63:895–905.

Fire, A., S. Xu, M.K. Montgomery, S.A. Kostas, S.E. Driver, and C.C. Mello. 1998. Potent and specific genetic interference by double-stranded RNA in *Caenorhabditis elegans*. *Nature*. 391:806–811.

Francis, G.R., and R.H. Waterston. 1985. Muscle organization in *Caenorhabditis elegans*: localization of proteins implicated in thin filament attachment and I-band organization. *J. Cell Biol.* 101:1532–1549.

Francis, R., and R.H. Waterston. 1991. Muscle cell attachment in *Caenorhabditis elegans*. *J. Cell Biol.* 114:465–479.

Fuchs, E., and D.W. Cleveland. 1998. A structural scaffolding of intermediate filaments in health and disease. *Science*. 279:514–519.

Fuchs, E., and Y. Yang. 1999. Crossroads on cytoskeletal highways. *Cell.* 98:547–550.

Gan, S.Q., O.W. McBride, W.W. Idler, N. Markova, and P.M. Steinert. 1990. Organization, structure, and polymorphisms of the human profilaggrin gene. *Biochemistry*. 29:9432–9440 (erratum published 30:5814).

Gatewood, B.K. 1996. Phenotypic, genetic and molecular analyses of the mup-4 gene in *Caenorhabditis elegans* demonstrate essential functions in maintenance of embryonic muscle position and hypodermal morphogenesis. Ph.D. thesis. University of Pennsylvania, Philadelphia. 140 pp.

Gatewood, B.K., and E.A. Bucher. 1997. The mup-4 locus in *Caenorhabditis elegans* is essential for hypodermal integrity, organismal morphogenesis and

embryonic body wall muscle position. *Genetics*. 146:165–183.

Goh, P.Y., and T. Bogaert. 1991. Positioning and maintenance of embryonic body wall muscle attachments in *C. elegans* requires the mup-1 gene. *Development*. 111:667–681.

Grant, B., and D. Hirsh. 1999. Receptor-mediated endocytosis in the *Caenorhabditis elegans* oocyte. *Mol. Biol. Cell*. 10:4311–4326.

Harding, C.R., and I.R. Scott. 1983. Histidine-rich proteins (filaggrins): structural and functional heterogeneity during epidermal differentiation. *J. Mol. Biol*. 170:651–673.

Haydock, P.V., C. Blomquist, S. Brumbaugh, B.A. Dale, K.A. Holbrook, and P. Fleckman. 1993. Antisense profilaggrin RNA delays and decreases profilaggrin expression and alters in vitro differentiation of rat epidermal keratinocytes. *J. Invest. Dermatol*. 101:118–126.

Henry, M.D., and K.P. Campbell. 1998. A role for dystroglycan in basement membrane assembly. *Cell*. 95:859–870.

Herz, J., U. Hamann, S. Rogne, O. Myklebost, H. Gausepohl, and K.K. Stanley. 1988. Surface location and high affinity for calcium of a 500-kd liver membrane protein closely related to the LDL-receptor suggest a physiological role as lipoprotein receptor. *EMBO J*. 7:4119–4127.

Houseweart, M.K., and D.W. Cleveland. 1998. Intermediate filaments and their associated proteins: multiple dynamic personalities. *Curr. Opin. Cell Biol*. 10:93–101.

Hresko, M.C., B.D. Williams, and R.H. Waterston. 1994. Assembly of body wall muscle and muscle cell attachment structures in *Caenorhabditis elegans*. *J. Cell Biol*. 124:491–506.

Hresko, M.C., L.A. Schriefer, P. Shrimankar, and R.H. Waterston. 1999. Myotactin, a novel hypodermal protein involved in muscle–cell adhesion in *Caenorhabditis elegans*. *J. Cell Biol*. 146:659–672.

Huang, X.Y., and D. Hirsh. 1989. A second trans-spliced RNA leader sequence in the nematode *Caenorhabditis elegans. Proc. Natl. Acad. Sci. USA*. 86:8640–8644.

Johnstone, I.L. 1994. The cuticle of the nematode *Caenorhabditis elegans*: a complex collagen structure. *Bioessays*. 16:171–178.

Johnstone, I.L. 2000. Cuticle collagen genes. Expression in *Caenorhabditis elegans. Trends Genet*. 16:21–27.

Jones, J.C., S.B. Hopkinson, and L.E. Goldfinger. 1998. Structure and assembly of hemidesmosomes. *Bioessays*. 20:488–494.

Kohara, Y. 1996. Large scale analysis of *C. elegans* cDNA. *Tanpakushitsu Kakusan Koso*. 41:715–720.

Kramer, J.M. 1997. Extracellular matrix. *In C. elegans* II. D.L. Riddle, T. Blumenthal, B.J. Meyer, and J.R. Priess, editors. Cold Spring Harbor Laboratory Press, Cold Spring Harbor, NY. 471–500.

Krause, M., and D. Hirsh. 1987. A trans-spliced leader sequence on actin mRNA in *C. elegans. Cell*. 49:753–761.

Kuechle, M.K., C.D. Thulin, R.B. Presland, and B.A. Dale. 1999. Profilaggrin requires both linker and filaggrin peptide sequences to form granules: implications for profilaggrin processing in vivo. *J. Invest. Dermatol*. 112:843–852.

Lee, J.O., P. Rieu, M.A. Arnaout, and R. Liddington. 1995. Crystal structure of the A domain from the α subunit of integrin CR3 (CD11b/CD18). *Cell*. 80:631–638.

Mancuso, D.J., E.A. Tuley, L.A. Westfield, N.K. Worrall, B.B. Shelton-Inloes, J.M. Sorace, Y.G. Alevy, and J.E. Sadler. 1989. Structure of the gene for human von Willebrand factor. *J. Biol. Chem*. 264:19514–19527.

Matsushima, M., M. Ichinose, N. Yahagi, N. Kakei, S. Tsukada, K. Miki, K. Kurokawa, K. Tashiro, K. Shiokawa, K. Shinomiya, et al. 1994. Structural characterization of porcine enteropeptidase. *J. Biol. Chem*. 269:19976–19982.

McArdle, K., T.S. Allen, and E.A. Bucher. 1998. Ca^{2+}-dependent muscle dysfunction caused by mutation of the *Caenorhabditis elegans* troponin T-1 gene. *J. Cell Biol*. 143:1201–1213.

Mello, C., and A. Fire. 1995. DNA transformation. *In Caenorhabditis elegans*: Methods in Cell Biology. Vol. 48. H. Epstein and D. Shakes, editors. Academic Press, San Diego, CA. 452–480.

Mello, C.C., J.M. Kramer, D. Stinchcomb, and V. Ambros. 1991. Efficient gene transfer in *C. elegans*: extrachromosomal maintenance and integration of transforming sequences. *EMBO J*. 10:3959–3970.

Mendoza, L.M., D. Nishioka, and V.D. Vacquier. 1993. A GPI-anchored sea urchin sperm membrane protein containing EGF domains is related to human uromodulin. *J. Cell Biol*. 121:1291–1297.

Miller, D.M., and D.C. Shakes. 1995. Immunofluorescence Microscopy. *In Caenorhabditis elegans*: Methods in Cell Biology. Vol. 48. H. Epstein and D. Shakes, editors. Academic Press, San Diego, CA. 365–389.

Moerman, D., and A. Fire. 1997. Muscle: structure, function and development. *In C. elegans* II. D. Riddle, T. Blumenthal, and J. Priess, editors. Cold Spring Harbor Laboratory Press, Cold Spring Harbor, NY. 417–470.

Mohler, W.A., J.S. Simske, E.M. Williams-Masson, J.D. Hardin, and J.G. White. 1998. Dynamics and ultrastructure of developmental cell fusions in the *Caenorhabditis elegans* hypodermis. *Curr. Biol*. 8:1087–1090.

Myers, C.D., P.Y. Goh, T.S. Allen, E.A. Bucher, and T. Bogaert. 1996. Developmental genetic analysis of troponin T mutations in striated and nonstriated muscle cells of *Caenorhabditis elegans*. *J. Cell Biol*. 132:1061–1077.

O'Guin, W.M., T.T. Sun, and M. Manabe. 1992. Interaction of trichohyalin with intermediate filaments: three immunologically defined stages of trichohyalin maturation. *J. Invest. Dermatol*. 98:24–32.

Plenefisch, J.D., X. Zhu, and E.M. Hedgecock. 2000. Fragile skeletal muscle attachments in dystrophic mutants of *Caenorhabditis elegans*: isolation and characterization of the mua genes. *Development*. 127:1197–1207.

Presland, R.B., P.V. Haydock, P. Fleckman, W. Nirunsuksiri, and B.A. Dale. 1992. Characterization of the human epidermal profilaggrin gene. Genomic organization and identification of an S-100-like calcium binding domain at the amino terminus. *J. Biol. Chem*. 267:23772–23781.

Priess, J.R., and D.I. Hirsh. 1986. *Caenorhabditis elegans* morphogenesis: the role of the cytoskeleton in elongation of the embryo. *Dev. Biol*. 117:156–173.

Rees, D.J., I.M. Jones, P.A. Handford, S.J. Walter, M.P. Esnouf, K.J. Smith, and G.G. Brownlee. 1988. The role of β-hydroxyaspartate and adjacent carboxylate residues in the first EGF domain of human factor IX. *EMBO J*. 7:2053–2061.

Resing, K.A., K.A. Walsh, J. Haugen-Scofield, and B.A. Dale. 1989. Identification of proteolytic cleavage sites in the conversion of profilaggrin to filaggrin in mammalian epidermis. *J. Biol. Chem*. 264:1837–1845.

Rogalski, T.M., B.D. Williams, G.P. Mullen, and D.G. Moerman. 1993. Products of the unc-52 gene in *Caenorhabditis elegans* are homologous to the core protein of the mammalian basement membrane heparan sulfate proteoglycan. *Genes Dev*. 7:1471–1484.

Rothnagel, J.A., and G.E. Rogers. 1986. Trichohyalin, an intermediate filament-associated protein of the hair follicle. *J. Cell Biol*. 102:1419–1429.

Sambrook, J., E.F. Fritsch, and T. Maniatis. 1989. Molecular Cloning: A Laboratory Manual. Cold Spring Harbor Laboratory Press, Cold Spring Harbor, NY. 1.42–1.43.

Sasaki, M., S. Kato, K. Kohno, G.R. Martin, and Y. Yamada. 1987. Sequence of the cDNA encoding the laminin B1 chain reveals a multidomain protein containing cysteine-rich repeats. *Proc. Natl. Acad. Sci. USA*. 84:935–939.

Sato, S. 1985. Ultrastructural localization of nucleolar material by a simple silver staining technique devised for plant cells. *J. Cell Sci*. 79:259–269.

Steinert, P.M., J.S. Cantieri, D.C. Teller, J.D. Lonsdale-Eccles, and B.A. Dale. 1981. Characterization of a class of cationic proteins that specifically interact with intermediate filaments. *Proc. Natl. Acad. Sci. USA*. 78:4097–4101.

Stewart, H.I., N.J. O'Neil, D.L. Janke, N.W. Franz, H.M. Chamberlin, A.M. Howell, E.J. Gilchrist, T.T. Ha, L.M. Kuervers, G.P. Vatcher, et al. 1998. Lethal mutations defining 112 complementation groups in a 4.5 Mb sequenced region of *Caenorhabditis elegans* chromosome III. *Mol. Gen. Genet*. 260:280–288.

Sulston, J.E., E. Schierenberg, J.G. White, and J.N. Thomson. 1983. The embryonic cell lineage of the nematode *Caenorhabditis elegans*. *Dev. Biol*. 100:64–119.

Titani, K., and K.A. Walsh. 1988. Human von Willebrand factor: the molecular glue of platelet plugs. *Trends Biochem. Sci*. 13:94–97.

Vidal, F., D. Aberdam, C. Miquel, A.M. Christiano, L. Pulkkinen, J. Uitto, J.P. Ortonne, and G. Meneguzzi. 1995. Integrin β4 mutations associated with junctional epidermolysis bullosa with pyloric atresia. *Nat. Genet*. 10:229–234.

von Heijne, G. 1986. A new method for predicting signal sequence cleavage sites. *Nucleic Acids Res*. 14:4683–4690.

Waterston, R.H. 1988. Muscle. *In* The Nematode *Caenorhabditis elegans*. W.B. Wood, editor. Cold Spring Harbor Laboratory, Cold Spring Harbor, NY. 281–335.

Williams, B.D., and R.H. Waterston. 1994. Genes critical for muscle development and function in *Caenorhabditis elegans* identified through lethal mutations. *J. Cell Biol*. 124:475–490.

Williams, B.D., B. Schrank, C. Huynh, R. Shownkeen, and R.H. Waterston. 1992. A genetic mapping system in *Caenorhabditis elegans* based on polymorphic sequence-tagged sites. *Genetics*. 131:609–624.

Williams-Masson, E.M., A.N. Malik, and J. Hardin. 1997. An actin-mediated two-step mechanism is required for ventral enclosure of the *C. elegans* hypo-

dermis. *Development*. 124:2889–2901.

Williams-Masson, E.M., P.J. Heid, C.A. Lavin, and J. Hardin. 1998. The cellular mechanism of epithelial rearrangement during morphogenesis of the *Caenorhabditis elegans* dorsal hypodermis. *Dev. Biol*. 204:263–276.

Wilson, R., R. Ainscough, K. Anderson, C. Baynes, M. Berks, J. Bonfield, J. Burton, M. Connell, T. Copsey, J. Cooper, et al. 1994. 2.2 Mb of contiguous nucleotide sequence from chromosome III of *C. elegans*. *Nature*. 368:32–38.

Yamagata, M., K.M. Yamada, S.S. Yamada, T. Shinomura, H. Tanaka, Y. Nishida, M. Obara, and K. Kimata. 1991. The complete primary structure of type XII collagen shows a chimeric molecule with reiterated fibronectin type III motifs, von Willebrand factor A motifs, a domain homologous to a noncollagenous region of type IX collagen, and short collagenous domains with an Arg-Gly-Asp site. *J. Cell Biol*. 115:209–221.

Yochem, J., and I. Greenwald. 1993. A gene for a low density lipoprotein receptor–related protein in the nematode *Caenorhabditis elegans*. *Proc. Natl. Acad. Sci. USA*. 90:4572–4576.

Yochem, J., T. Gu, and M. Han. 1998. A new marker for mosaic analysis in *Caenorhabditis elegans* indicates a fusion between hyp6 and hyp7, two major components of the hypodermis. *Genetics*. 149:1323–1334.

Yochem, J., S. Tuck, I. Greenwald, and M. Han. 1999. A gp330/megalin-related protein is required in the major epidermis of *Caenorhabditis elegans* for completion of molting. *Development*. 126:597–606.